Astron. Astrophys. 335, 539–544 (1998)

ASTRONOMY AND ASTROPHYSICS

# Milliarcsecond radio structure of LS I +61°303

**J.M. Paredes**[1], **M. Massi**[2,3], **R. Estalella**[1], **and M. Peracaula**[1,4]

[1] Departament d'Astronomia i Meteorologia, Universitat de Barcelona, Av. Diagonal 647, E-08028 Barcelona, Spain
[2] Joint Institute for VLBI in Europe. Postbus 2, 7990 AA Dwingeloo, The Netherlands
[3] Max-Planck-Institut für Radioastronomie, Auf dem Hügel 69, D-53121 Bonn, Germany
[4] Department of Physics and Astronomy, University of Calgary, 2500 University Dr. NW, Calgary, Alberta, T2N 1N4, Canada

Received 2 December 1997 / Accepted 7 April 1998

**Abstract.** We present results of two-epoch intercontinental VLBI observations at 6 cm wavelength of LS I +61°303 during an outburst in 1993. In the first epoch, the total flux density of LS I +61°303 varied from 76 to 131 mJy and the derived size of the emitting region was about 3 mas. In the second epoch, four days later, the flux density of LS I +61°303 was very stable, at a level of 60 mJy. The flux stability along all the second session allowed us to carry out standard hybrid mapping. The VLBI map obtained exhibits an extended structure of about 7 mas with an unresolved component at the center of the extended structure. The results derived from both observing sessions seem to agree with a source expanding with time from 2–3 to 7 mas, at a velocity of $\sim$2200 km s$^{-1}$. In addition, our results suggest the existence of a quiescent component associated with the core.

**Key words:** stars: individual: LS I +61°303 – stars: variables: other – radio continuum: stars – X-rays: stars – techniques: interferometric

## 1. Introduction

LS I +61°303 is a Be massive X-ray binary system and one of the most unusual objects in the Galaxy. It presents periodic radio outbursts, of variable amplitude, with a period $\sim$26.5 days (Taylor & Gregory 1982, 1984), assumed to be coincident with the orbital period of the system. At radio wavelengths, two more periodicities, longer and shorter than the 26.5 d have been found. Occasional evidence of a short term period of 1.4 hours with a few mJy amplitude has been reported by Peracaula et al. (1997a). A long-term $\sim$4 year period modulation of the peak amplitude radio outburst, has been claimed by Paredes (1987) and Gregory et al. (1989). The existence of this modulation, with a period of 1598 d, seems to be confirmed by Peracaula (1997).

At optical and infrared wavelengths, a similar 26.5 d periodic behavior has been reported as well (Mendelson & Mazeh 1989; Paredes et al. 1994). Spectroscopic radial velocity observations are in agreement with the 26.5 d radio period, and indicate a rapidly rotating B0 V star, with an equatorial disk and mass loss (Hutchings & Crampton 1981), and a low mass secondary (1.1–1.5 $M_{\odot}$). The system is an X-ray source (Bignami et al. 1981), and recently, Paredes et al. (1997) found evidence that X-ray outbursts in LS I +61°303 are very likely to recur with the same radio outburst period. At higher energies, LS I +61°303 is suspected of being associated with the $\gamma$-ray source CG135+01 (Hermsen et al. 1977). Modern COMPTON GRO observations (Fichtel et al. 1994, Tavani et al. 1996) are consistent with a positional coincidence.

The radio outburst emission of LS I +61°303 is usually interpreted as non-thermal synchrotron radiation from relativistic electrons. Multi-frequency radio observations carried out throughout a full orbital cycle (Hjellming & Han 1995; Paredes et al. 1996) and the detection of linear polarization in LS I +61°303 (Peracaula et al. 1997a) give observational support to this interpretation. The radio emission is optically thin between 3.6 and 6 cm, even during the onset of the radio outburst. As suggested by Taylor & Gregory (1984) and modeled by Paredes et al. (1991), this behavior is consistent with continuous injection of relativistic electrons in order to account for the flux density rise at optically thin frequencies. Various possible models of the origin and/or time evolution of the relativistic electron population have been proposed. Maraschi & Treves (1981) propose that radio emitting particles responsible for the radio outbursts are produced in the interacting region between the relativistic wind of the compact companion (a pulsar) and the normal wind of the primary star. Lipunov & Nazin (1994) model the radio light curves expected when these relativistic electrons are captured by the magnetosphere of the primary star. Alternatively, the model proposed by Taylor & Gregory (1982, 1984) and revised by Taylor et al. (1992), consider that the time evolution and spectrum of the radio outburst are consistent with multiple blast waves caused by supercritical accretion events onto a compact companion. Assuming supercritical accretion events, Martí & Paredes (1995) develop an scenario which tries to provide a multiwavelength understanding of this object.

LS I +61°303 was observed with VLBI techniques by Lestrade et al. (1988) during its quiescent state (25 mJy) at 1.6 GHz yielding a source size of 4 mas. It is not clear if this source size is due to interstellar scattering. By extrapolating the 1.6 GHz measurements to 5 GHz, a size of 0.4 mas for interstellar scattering is obtained. At this frequency Taylor et al. (1992)

*Send offprint requests to*: J.M. Paredes

observed LS I +61°303 using the EVN and obtained an angular size of $3.2 \pm 0.9$ mas by fitting a single circular Gaussian to the data. Massi et al. (1993) obtained the first high resolution map of LS I +61°303 during the active radio emission (200 mJy) at 5 GHz, showing two components separated by 0.9 mas, with a source overall size of $\sim$1.6$\times$1.0 mas. Recently, Peracaula et al. (1997b) presented the first VLBI images of the quiescent emission. Their results indicate that the source was experiencing a mini-flare during the observing time. This flare occurred on milliarcsecond scales and it was associated with an increase of the compact radio structure size at velocity $\sim 0.06\ c$.

In this paper, we present new results obtained from global VLBI observations of LS I +61°303 carried out at two different orbital phases, in order to obtain a direct estimation of the projected expansion velocity as well as the possible geometric variations. From the known average radio light curves of LS I +61°303 for the active phase and the quiet phase (Paredes et al. 1990), we could select the observing dates to coincide as close as possible with the active and the decaying states of the radio outburst.

## 2. Observations and data reduction

LS I +61°303 was observed with a 7-element VLBI array at 6 cm wavelength on 1993 September 9 and 13 during two runs of about 12 hours each. The antennas used are listed in Table 1. The data were recorded using the Mark III recording system (Rogers et al. 1983) mode B (28 MHz) and correlated on the Mark III correlator operated by the Max-Planck-Institut fur Radioastronomie in Bonn.

Data were edited and calibrated using the measured system temperature and antenna gain curves. In Table 1 we give the ratios of the average system temperatures over the gains for each telescope (the so called SEFD factor, Source Equivalent Flux Density). Hardware errors at Westerbork during the whole VLBI session made the observations much less sensitive than normal and we have taken out these data. The VLBI calibrator was 0224+671 (4C67.05). As VLA calibrators we used 1331+305 and 0137+331 for the amplitude, and 0224+671 was also used for the phase.

In addition to the phased array mode for VLBI experiments, we used the normal interferometer output of the VLA interferometer of NRAO[1] to obtain the total flux densities during the VLBI experiment. The flux density variations of LS I +61°303 during the two observing sessions are shown in Fig. 1. The dates of the sessions were selected to coincide close with the peak of a radio outburst and with its decaying state. However, the time of the peak radio flux, which usually occurs at radio phase 0.6, can be predicted within about $\pm$2 days (Paredes et al. 1990). The radio phase of the first session was 0.66 and that of the second session was 0.81, being both calculated according to the period of 26.496 d and phase zero at Julian Date 2443366.775 (Taylor & Gregory 1984).

[1] The NRAO is operated by Associated Universities, Inc., under cooperative agreement with the National Science Foundation.

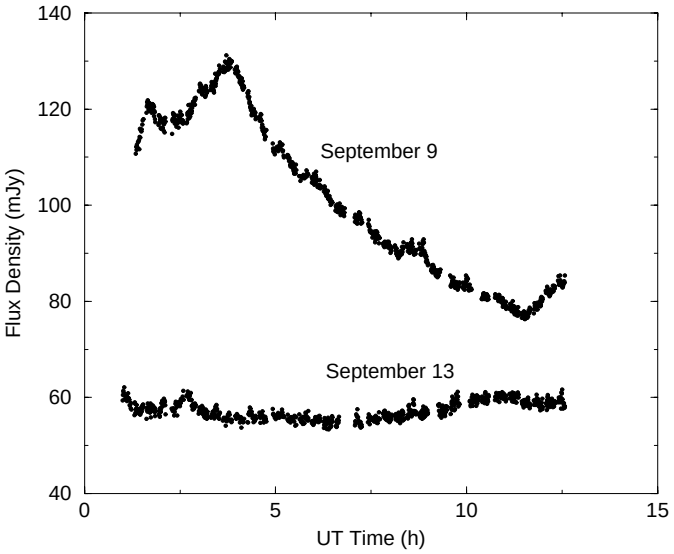


**Fig. 1.** Flux density variations of LS I +61°303 obtained from the VLA, with a time resolution of 30 seconds during the VLBI observation. The plots correspond to the observing sessions of 1993 September 9 (*upper*) and of 1993 September 13 (*lower*). The rms of each data point is typically 1 mJy or less. The data are thoroughly discussed in Peracaula et al. (1997a)

**Table 1.** Antennas used

| Antenna | Location | SEFD (Jy) | Diameter (m) |
|---|---|---|---|
| Effelsberg | Bonn, Germany | 52 | 100 |
| Jodrell2 | Jodrell Bank, U.K. | 433 | 25 |
| Medicina | Bologna, Italy | 355 | 32 |
| Noto | Noto, Italy | 313 | 32 |
| Onsala85 | Onsala, Sweden | 770 | 25 |
| VLBA-OV | Owens Valley, California | 464 | 25 |
| Phased VLA | Socorro, New Mexico | 22 | 27$\times$25 |

During the first session (September 9) the flux density changed significatively, varying from 76 to 131 mJy. In order to minimize the effect of time variations, we segmented the VLBI data in three sets with reliable flux density stability in each one. The time range of each dataset, identified as Parts A, B and C, are shown in Fig. 2. The $(u, v)$ coverage for each dataset is shown in Fig. 3. As can be seen, the visibilities are distributed along a different preferential direction for each part. Therefore, the direction of the highest angular resolution will be different for each part.

In the second session (September 13) the flux density of LS I +61°303 was very stable, at a level of $\sim$60 mJy. We could therefore use the whole data set, with the $(u, v)$ coverage shown in the bottom right corner of Fig. 3.

## 3. Results

### *3.1. September 9 run*

The limited $(u, v)$ coverage of Parts A, B and C of September 9 prevented us from reliable mapping. Instead, model fitting

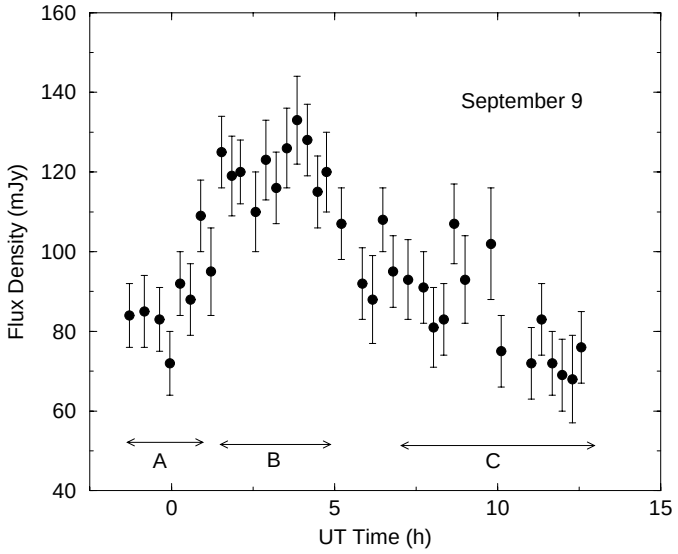


**Fig. 2.** Flux density of LS I +61°303 obtained from the Effelsberg antenna during the September 9 VLBI observation. The horizontal arrows show the different time ranges during which the emission level could be considered roughly constant.

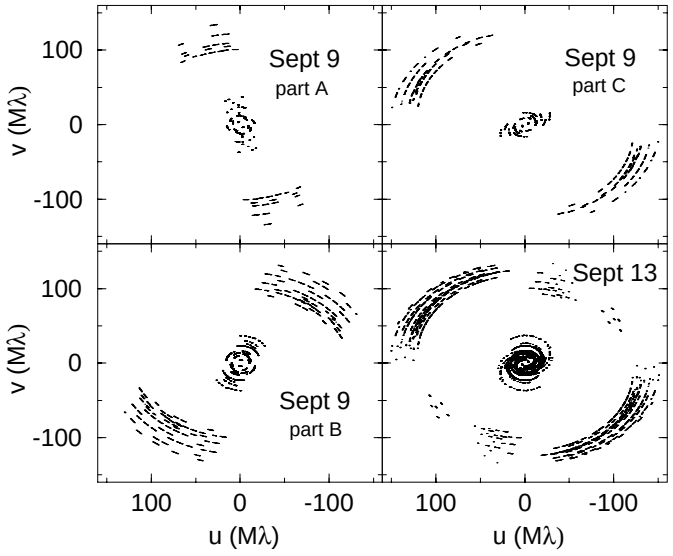


**Fig. 3.** Coverage in the $(u, v)$ plane for the separate VLBI datasets A, B and C of September 9, and of September 13.

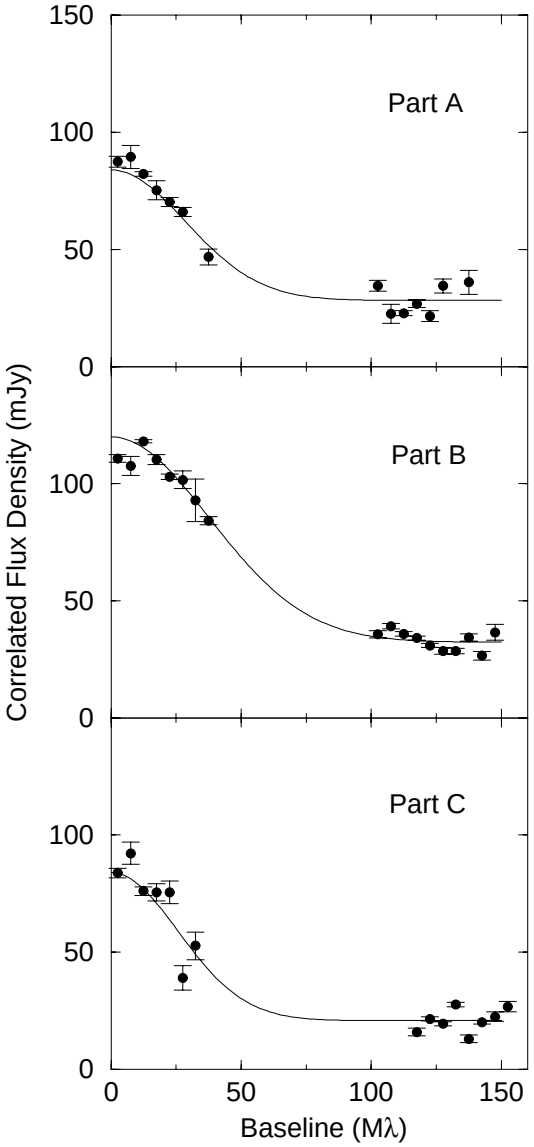


**Fig. 4.** Correlated flux density as a function of baseline for each dataset of September 9. The solid lines represent the fit of a circular Gaussian halo plus an unresolved core to the data, with a total flux density equal to that measured by the Effelsberg antenna.

techniques had to be used on the visibility data. In Fig. 4 the amplitude versus baseline spacing is shown for each of the three data sets. The data have been averaged in bins of $(u, v)$ radius of 5 M$\lambda$. The error bars are the rms error of the average in the bin. The model fitted is an unresolved core plus a circular Gaussian halo with a total flux equal to the flux measured by the Effelsberg antenna. The best fit for all data sets was obtained for an halo FWHM of 2–3 mas and the unresolved core contributing for at least one fourth of the total flux. The fitted values are given in Table 2 and the best fit is drawn as a solid line in Fig. 4.

By assuming a distance of 2.3 kpc for LS I +61°303 (Gregory et al. 1979) we can derive the linear size for each data set (see Table 2). If we compare the size obtained, $\sim$6 AU, with the semimajor axis of the orbit (0.40 AU or 0.17 mas at 2.3 kpc, assuming a primary B star of 10 $M_{\odot}$), we see that the source size is one order of magnitude greater than the binary system separation.

The size of the emitting region and the observed flux density (core plus halo) allow us to estimate the brightness temperature, using the relation

$$T_{\rm B} = 1.77 \times 10^9 \left(\frac{\nu}{\rm GHz}\right)^{-2} \left(\frac{S}{\rm mJy}\right) \left(\frac{\theta}{\rm mas}\right)^{-2},$$

where $S$ is the flux density and $\theta$ the angular size of the source. The value obtained for the brightness temperature, $T_{\rm B} \simeq 10^9$ K (see Table 2), is characteristic of non-thermal emission.

**Table 2.** Flux density, size and brightness temperature of LS I +61°303

| | | | Unresolved Core | | Gaussian Halo | | | |
|---|---|---|---|---|---|---|---|---|
| | | | Flux | Brightness | Flux | | Linear | Brightness |
| | Radio | | Density | Temperature[a] | Density | FWHM | Size | Temperature |
| Date | Phase | Dataset | (mJy) | ($10^9$K) | (mJy) | (mas) | (AU) | ($10^8$K) |
| 1993 Sep 9 | 0.66 | A | 28 | $\gg 1.2$ | 56 | 2.7 | 6.2 | 8.2 |
| | | B | 32 | $\gg 1.4$ | 88 | 2.1 | 4.8 | 19.3 |
| | | C | 21 | $\gg 0.9$ | 63 | 3.0 | 6.9 | 6.6 |
| 1993 Sep 13 | 0.81 | | 25 | $\gg 1.1$ | 35 | 7.1 | 16.3 | 0.8 |

[a] Lower limit estimated using the size of the beam.

### *3.2. September 13 run*

The flux density stability along the whole second session allowed us to have enough $(u, v)$ coverage to attempt hybrid mapping. However, before mapping, we fitted a core-halo structure to the data averaged in bins of $(u, v)$ radius of 5 M$\lambda$ and with the total flux equal to the flux measured by the Effelsberg antenna. The best values obtained for the size and flux density are reported in Table 2, together with the derived linear size and brightness temperature. The flux is equally distributed between the resolved and the unresolved components. In Fig. 5, the correlated flux density versus baseline is plotted, the solid line being the best fit.

The hybrid map was made using, independently, both the NRAO AIPS and the Caltech DIFMAP packages, obtaining practically the same image. The final VLBI map, restored with a beam size of 1.5×1.1 mas (PA=$-57°$) is shown in Fig. 6. We remind here that the interstellar scattering could produce at our observing frequency a maximum scattering size of 0.4 mas, much smaller than our measurements . This result is consistent with the previous fitting on the visibilities. The map exhibits an extended structure of about 6 mas, and an unresolved component at the center of the extended structure. The total flux of the map is 50 mJy. The VLA flux density for this epoch is ∼10 mJy greater than this value. This suggests the presence of a larger structure not sampled with our VLBI spacings.

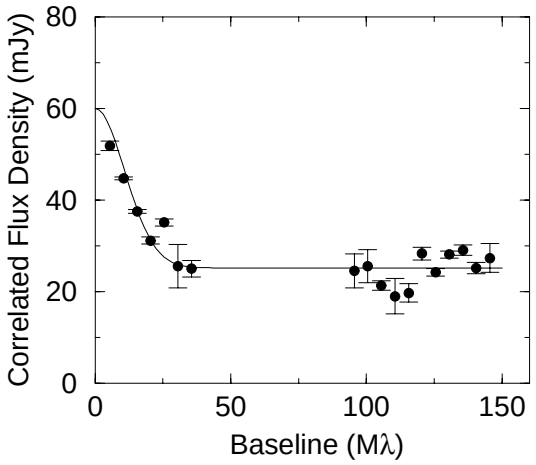


**Fig. 5.** Correlated flux density as a function of baseline for September 13. The solid line represents the fit of a circular Gaussian halo plus an unresolved core to the data, with a total flux density equal to that measured by the Effelsberg antenna.

## 4. Discussion

The data analysis of the two-epoch VLBI observations shows that the radio emission of LS I +61°303 can be modeled with two components. The two components seem to have a rather different nature: one compact and steady in flux density (within the two epochs), and the other resolved, expanding and fading away.

### *4.1. Compact component*

During the first run the flux density of the compact component has values of 28 mJy, 32 mJy (at the flare maximum), and 21 mJy. Four days later the flux density of this component is still 25 mJy. In other words, there seems to exist a stable level of emission around $25 \pm 4$ mJy before the flare maximum, immediately after it, and still four days later, with a flare maximum value of 32 mJy barely outside the error bar. By averaging the most longer baselines data through all four data sets (3 of the first run and 1 of the second run) we would obtain a total flux density of $27 \pm 6$ mJy for this core component. Where does this nearly stable component come from, and why does it not seem to participate in the flaring process? We remind here that the emission in LS I +61°303 consists in an active phase between 0.4 and 1.0 of radio phase (restricted to 0.6–0.8 when only the larger outbursts are considered) and a quiescent phase. Peracaula et al. (1997b) advanced the hypothesis that the "quiescent" low level radio emission of LS I +61°303 is not simply due to the slow decay of the radiation of the large outbursts. These authors found evidence of a small amplitude flare during the quiescent phase, whose brightening is accompanied by an increase in size (of a compact component) with a velocity of $0.06\ c$. After reaching a size of ∼2 mas the expansion stops and the flux density drops to the value it had before the mini flare. In other words there could exist a sort of mini flare mechanism able to maintain a "quiescent" level. Our finding of a quiescent component during the flaring phase implies that the mechanism producing mini flares is always active, not only during the quiescent phase, but also co-existent with the much larger outbursts. It is therefore a mechanism completely independent from that producing the larger flares.

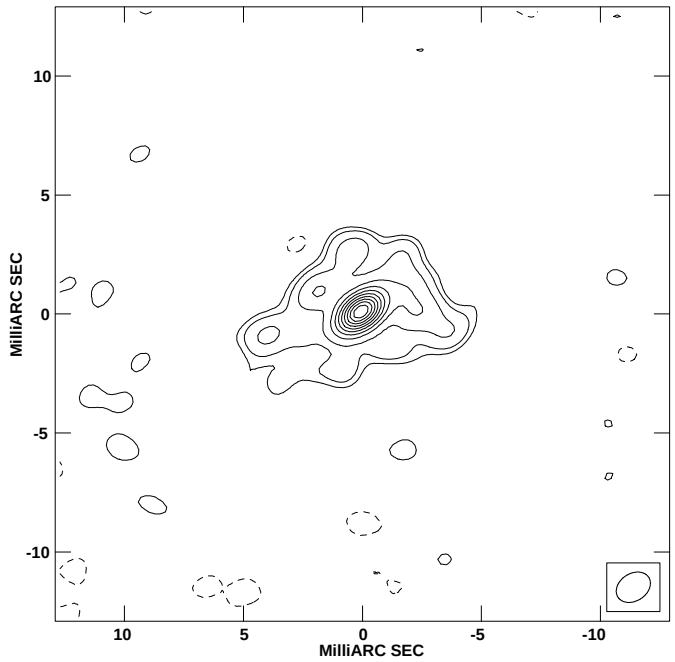


**Fig. 6.** Hybrid map of LS I +61°303 obtained from the data of 1993 September 13. The restoring beam, 1.5×1.1 mas at 57°, is shown in the lower right corner. The map peak is 16.8 mJy/beam. The contour levels displayed are −3, 3, 5, 10, 20, 30, 40, 50, 60, 70, 80 and 90% of the peak.

It is interesting to compare the level of the quiescent emission observed so far with the flux density of our compact component. Paredes et al. (1990) determined at 3.6 cm a quiescent level slightly modulated, reaching a minimum of 18 mJy. The daily monitoring of Ray et al. (1997) during the last 3 years with the Green Bank Interferometer at 13 cm and 3.6 cm wavelength, gives a quiescent average flux density of 30 mJy and 20 mJy respectively. The level of the quiescent component in the Peracaula et al. (1997b) observation is around 15 mJy at VLBI scales and between 22–35 mJy at VLA scales. The value of $27 \pm 6$ mJy we found for the compact component is therefore consistent with the values measured up to now during the quiescent phase.

### *4.2. Extended component*

In the first run the extended component is 2–3 mas in size and has an average flux density of ∼70 mJy. In the second run, four days later, it has reached size of 7 mas and has a flux density of 35 mJy. The resulting expansion velocity, by taking the difference between the two half-widths of the halo, is ∼0.56 mas d$^{-1}$, equivalent to 2200 km s$^{-1}$ or $0.0075\ c$. This value is a factor five greater than the speeds inferred by Taylor et al. (1992) and Massi et al. (1993). However, these authors had only one observing epoch and they only could estimate the velocity by indirect arguments assuming that the material they observed had been ejected some days before. On the other hand, our expansion velocity is a factor 8 lower than the value of ∼0.06 $c$ found by Peracaula et al. (1997b) for sizes less than 2 mas.

The 2200 km s$^{-1}$ expansion velocity measured directly from our VLBI observations is consistent with the supercritical accretion model proposed by Taylor & Gregory (1984), which predicts that radiating electrons must travel outward from the system at velocities in excess of 1000 km s$^{-1}$ in order to avoid catastrophic inverse Compton losses by nearby optical primary photons. The increase in size and simultaneous decay in intensity agree with that expected for an optically thin cloud of relativistic electrons expanding adiabatically.

Regarding the geometry of the source, as was said in Sect. 3.1, we cannot produce a reliable map for the September 9 data. However, as our source size estimation of 2–3 mas (see Table 2) agrees with the size of about 2 mas obtained by Massi et al. (1993) for a similar orbital phase (0.70 as compared with 0.66), we can assume that this day the source had a similar shape to that in Massi et al. (1993). Our map of September 13 shows a source large in size and roughly circular. The Massi et al. (1993) map, with a higher angular resolution, shows two sources, both almost confined in the compact component of our present lower resolution map of Fig. 6. By analogy to other X-ray binaries like SS433 and Cygnus X-3, one should rather expect a radio structure with jet-like morphology, and possibly not with the roughly circular shape in the map of Fig. 6. Our map seems to indicate that the outflow is not well collimated and the that the jet has an initial large opening angle.

## 5. Conclusion

As a conclusion from our two-epoch VLBI observations, a temptative scenario of the radio emission of LS I +61°303 can be described as follows.

Two independent process seem to be at work in LS I +61°303. One process, the strongest at radio wavelengths, takes place around phase 0.6. The ejection of matter is jet-like, but the opening angle seems to be larger than in similar objects, and the expansion velocity rather small, ∼2200 km s$^{-1}$, almost a factor 20 smaller than in SS433 (Vermeulen et al. 1993) or Cygnus X-3 (Schalinski et al. 1995). The size of the emitting region is one order of magnitude greater than the separation of the binary system. Any initial elongation in the shape of the source is lost quite soon and the source displays a roughly circular shape only four days after the flare.

The second is a mini flaring process, always active and able to maintain a quiescent level of 15–26 mJy at 6 cm (Peracaula et al. 1997a). The ejection velocity is in this case $0.06\ c$. The origin of these mini flares could be luminosity-driven shocks (Taylor & Gregory 1984). Each shock should clear the volume inside the binary system in a shorter time scale than the blast repetition rate. This could explain the initial high velocity of expansion. When reaching a size of ∼2 mas the electrons should run in some more slowly expanding material created in the larger outburst. This mini flaring process is responsible for the nearly steady core component detected in our observations

*Acknowledgements.* We thank the correlator staff at MPIfR in Bonn for help during the correlation of the data. We thank Scott Aaron for

interesting discussions. MP acknowledges financial support from the Spanish Ministerio de Educación y Ciencia. JMP, RE and MP acknowledge partial support from DGICYT grant PB94-0904. We acknowledges support for this research by the European Union under contract CHGECT20011. Moreover MM acknowledges support for her research by the European Union under contract FMGECT950012

## References

Bignami G.F., Caraveo P.A., Lamb R.C., Markert T.H., Paul J.A., 1981, ApJ 247, L85
Fichtel C.E., Bertsch D.L., Chiang J., et al., 1994, ApJS 94, 551
Gregory P.C., Taylor A.R., Crampton D., et al., 1979, AJ 84, 1030
Gregory P.C., Huang-Jian Xu, Backhouse C.J., Reid A., 1989, ApJ 339, 1054
Hermsen W., Swanenburg B.N., Bignami G.F. et al., 1977, Nat 269, 495
Hjellming R.M., Han X., 1995, in *X-Ray Binaries*, Cambridge Astrophysics Series 26, 308
Hutchings J.B., Crampton D., 1981, PASP 93, 486
Lestrade J.-F., 1988, in *The Impact of VLBI on Astrophysics and Geophysics*, M.J. Reid and J.M. Moran Eds., Kluwer, Boston, 265
Lipunov V.M., Nazin S.N., 1994, A&A 289, 822
Maraschi L., Treves A., 1981, MNRAS 194, 18
Martí J., Paredes J.M., 1995, A&A 298, 151
Massi M., Paredes J.M., Estalella R., Felli M., 1993, A&A 269, 249
Mendelson H., Mazeh T., 1994, MNRAS 267, 1
Paredes J.M., 1987, PhD Thesis, Universitat de Barcelona
Paredes J.M., Estalella R., Rius A., 1990, A&A 232, 377
Paredes J.M., Martí J., Estalella, R., Sarrate, J., 1991, A&A 248, 124
Paredes J.M., Marziani P., Martí J., et al., 1994, A&A 288, 519
Paredes J.M., Martí J., Fabregat J., et al., 1996, in *Radio Emission from the Stars and the Sun*. A.R. Taylor & J.M. Paredes Eds., ASP Conference Series, Vol. 93, 243
Paredes J.M., Martí J., Peracaula M., Ribó M., 1997, A&A 320, L25
Peracaula M., 1997, PhD Thesis, Universitat de Barcelona
Peracaula M., Martí J., Paredes J.M., 1997a, A&A 328, 283
Peracaula M., Gabuzda D.C., Taylor A.R., 1997b, A&A 330, 612
Ray P.S., Foster R.S., Waltman E.B., Ghigo F.D., Tavani M., 1997, ApJ 491, 381
Rogers A.E.E., Cappallo R.J., Hinteregger H.F., et al., 1983, Sci. 219, 51
Schalinski C.J., Johnston K.J, Spencer R.E., et al., 1995, ApJ 447, 752
Tavani M., Hermsem W., van Dijk R., et al., 1996, A&AS 120, 243
Taylor A.R., Gregory P.C., 1982, ApJ 255, 210
Taylor A.R., Gregory P.C., 1984, ApJ 283, 273
Taylor A.R., Kenny H.T., Spencer R.E., Tzioumis A., 1992, ApJ 395, 268
Vermeulen R.C., Schilizzi R.T., Spencer R.E., Romney J.D., Fejes I., 1993, A&A 270, 177